



Contents lists available at ScienceDirect

## International Journal of Solids and Structures

journal homepage: [www.elsevier.com/locate/ijsolstr](http://www.elsevier.com/locate/ijsolstr)

## Statics of elastic cables under 3D point forces

Nicola Impollonia<sup>a,\*</sup>, Giuseppe Ricciardi<sup>b</sup>, Fernando Saitta<sup>a</sup><sup>a</sup> Dipartimento DARC, Università di Catania, P.zza Federico di Svevia, 96100 Siracusa, Italy<sup>b</sup> Dipartimento di Ingegneria Civile, Università di Messina, C.da di Dio, 98166 Villaggio S. Agata, Messina, Italy

## ARTICLE INFO

## Article history:

Received 17 September 2010

Received in revised form 30 November 2010

Available online 11 January 2011

## Keywords:

Cable structures

Elastic catenary

Closed form solution

Non-planar cable layout

## ABSTRACT

The catenary problem for elastic cables is extended to the case of uniformly distributed loads and point forces however oriented in space. The equilibrium equation is written in vector form and its solution, i.e. the deformed shape of the elastic cable, is obtained in closed form for the cases of uniformly distributed load, one point force and many point forces. The formulation is suitable to solve straightforwardly cable structure problems, as shown in the numerical applications.

© 2011 Elsevier Ltd. All rights reserved.

## 1. Introduction

The circumstance that a chord under self-weight is unable to maintain its rectilinear configuration, in spite of the tension which can be applied at its ends, was known already in 1638 by Galileo Galilei; however, in Galilei opinion the configuration of the chord was parabolic, in accordance with the flight path of a projectile (Galilei, 1638). The mathematical treatment of the cable theory began in the latter half of the seventeenth century. The initial problem was to determine the equilibrium position of an inextensible string hanging between two points and subjected to various load conditions. In particular, the *catenary problem* consists in finding the equilibrium shape of the cable under self-weight. The non-parabolic shape of the chord was noted by Jungius in 1669 but he was not able to find out the real mathematical expression of the curve. The problem was proposed by Jakob Bernoulli in the *Acta Eruditorum* (Bernoulli, 1691) and, after this date, was tackled and solved separately by Huygens, via pure geometric considerations, and by Leibniz (Bernoulli, 1692; Leibniz, 1691a,b) and Johann Bernoulli, Jakob's brother, via the integral calculus. All the three solutions were published in the *Acta* (Leibniz, 1691a,b). The name *catenary* it seems was due to Huygens, who used it in 1690 in a letter to Leibniz.

All the mentioned works did not take into account cable extensibility. The Hooke's law was postulated in 1675 as an anagram (Hooke, 1675; Kurrer, 2008) and clearly written in 1678 (Hooke, 1678). After these dates, Bernoulli brothers were the first who formulated the differential equation of equilibrium of the elastic cable, following the law postulated by Hooke. Also

Euler contributed to the study on the catenary, after a suggestion of Daniel Bernoulli; he uses the variation calculus (the "method of final causes") and shows that the equilibrium configuration is determined by the lowest position of the barycentre of mass, i.e. by the minimum of potential energy of the gravity forces (Euler, 1744; Timoshenko, 1983). From an engineering point of view, the mathematical theory of cables allowed to define rules based on analytical reasoning for the design of suspension bridges (Navier, 1823).

Although the analytical expression for the solution of the elastic catenary is nowadays well known and represents the basis of classical literature on cable structures (O'Brien, 1967; Irvine, 1981), it seems worthy to extend the standard solution, confined to the case of loads acting on the plane of the cable, to more general load conditions. Indeed, after some centuries the interest in the subject remains still relevant as cables are widely used in structural engineering. Even if a major effort has been devoted by researchers to numerical cable dynamics and computational methods seem to allow the solution of any problem, closed form solutions still preserve an important role as they allow a drastic reduction of computational effort, a deeper understanding of the structural behavior and serve as benchmark solutions for numerical procedures. For static setting, the exact solution for an elastic cable with distributed or concentrated vertical loads has been given in the work by Irvine and Sinclair (1976), about two centuries after the discovery of the static solution under self-weight. If the parabolic approximation can be accurate for low sagged cables, the exact solution must be preferred for more general case (inclined cables and/or spatial load conditions). In addition the computational advantage of using approximate solutions is not an issue with nowadays computers so that, recent papers (Lepidi et al., 2007; Such et al.,

\* Corresponding author.

E-mail address: [nimpo@unict.it](mailto:nimpo@unict.it) (N. Impollonia).

2009; Huang and Lan, 2006; Andreu et al., 2006) make use of the catenary equation for solving the static cable problem.

In this paper, the solution proposed in Irvine's book (Irvine, 1981) for the static analysis of the elastic cable is extended to three dimensions so to treat point forces and uniformly distributed load anyway oriented in space, acting in the unstrained configuration. The solution is cast in a compact vector form easy to handle even for the case of many point forces, so to manage practical engineering problems.

The first part of the paper is dedicated to the derivation of the solution for a generally oriented uniformly distributed load. The inclusion of a point force arbitrarily oriented in space is then considered. Finally, the setting with many point forces is analysed and thermal loads are introduced. A model validation is carried out checking consistency with standard solution and assessing the capability to predict out of plane displacements.

Two numerical applications are presented, related to a cable net and a transport pulley system. The cable net, already treated by other authors (Such et al., 2009; Huang and Lan, 2006; Peyrot and Goulois, 1979) in the case of vertical loads only, is subjected to a wind load which induces inclined cable configurations. The transport pulley system, analysed by Such et al. (2009) and Bruno and Leonardi (1999) under self-weight, is also studied in a three dimensional configuration giving a complete description of its structural behavior.

## 2. Extensible cables with uniformly distributed load

The catenary equation for extensible cables, assuming perfect shear and bending flexibility, will be derived in this paragraph according to Hooke's law. Following the analytical treatment adopted by Irvine (1981), the three dimensional case of uniformly (and non-segmented) distributed load acting in the unstrained configuration, in any direction in space, will be considered herein.

With reference to Fig. 1, the Lagrangian coordinate  $\ell$  represents the length of the unstrained cable (configuration C) between the generic point and the cable origin. The figure assumes that cable origin coincides with the origin of the reference system although this may not be case, as for cable nets or 3D cable systems. Denoting with  $L$  the unstrained cable length, it will be  $0 \leq \ell \leq L$ . If the equilibrium of the cable segment between the cable origin and the point with abscissa  $\ell$  is considered with reference to the stretched state (configuration C\*), the following equation is obtained:

$$\mathbf{T}(\ell) = \mathbf{R} - \mathbf{p}\ell \tag{1}$$

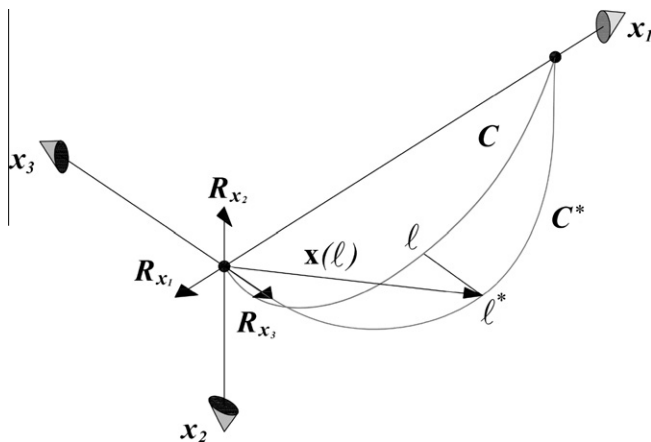


Fig. 1. Unstrained configuration C and stretched configuration C\* under uniformly distributed load.

where  $\mathbf{R} = [R_{x_1}, R_{x_2}, R_{x_3}]^T$  is the vector collecting the reaction forces at cable origin and  $\mathbf{p} = p\boldsymbol{\pi}$  is the vector of distributed load with constant intensity  $p$  acting along the cable in the direction defined by the versor  $\boldsymbol{\pi}$ . Moreover:

$$\mathbf{T}(\ell) = T(\ell)\boldsymbol{\tau}(\ell) \tag{2}$$

is the cable tension vector, parallel to the tangent versor in the stretched configuration C\*, given as

$$\boldsymbol{\tau}(\ell) = \frac{d\mathbf{x}(\ell)}{d\ell^*} \tag{3}$$

In the previous equation  $\mathbf{x}(\ell) = [x_1(\ell), x_2(\ell), x_3(\ell)]^T$  is the vector defining the stretched configuration C\* of the cable and  $\ell^* = \ell^*(\ell)$  is the length of the cable segment in the stretched configuration (see Fig. 1). It is worth noticing that the coordinate function  $\mathbf{x}(\ell)$  has the peculiarity to univocally locate the position (in the deformed configuration) of a material point defined by the curvilinear abscissa  $\ell$  in the unstrained configuration.

The cable tension  $T(\ell)$  is obtained by taking the norm of the two sides of Eq. (1):

$$T(\ell) = \|\mathbf{R} - \mathbf{p}\ell\| \tag{4}$$

With a view to the concise exhibition of the solution, the following quantities relative to non-dimensional forces are introduced:

$$\mathbf{r} = \frac{\mathbf{R}}{pL}; \quad \mathbf{t}(\ell) = \frac{\mathbf{T}(\ell)}{pL} \tag{5a, b}$$

In particular,  $\mathbf{r}$  is the vector of the dimensionless reaction forces at cable origin and  $t(\ell) = \|\mathbf{t}(\ell)\| = T(\ell)/(pL)$  is the dimensionless cable tension.

Adopting dimensionless coordinates

$$s = \frac{\ell}{L}; \quad s^* = \frac{\ell^*}{L} \tag{6a, b}$$

and introducing the dimensionless position vector

$$\boldsymbol{\xi}(s) = \frac{\mathbf{x}(sL)}{L} \tag{7}$$

with  $0 \leq s \leq 1$ , the equilibrium Eq. (1) may be rewritten as follows:

$$\mathbf{t}(s) = t(s) \frac{d\boldsymbol{\xi}(s)}{ds^*} = \mathbf{r} - \boldsymbol{\pi}s \tag{8}$$

so that

$$t(s) = \|\mathbf{r} - \boldsymbol{\pi}s\| \tag{9}$$

With the aim of evaluating the stretched configuration, the Hooke's law is considered:

$$T(\ell) = EA \frac{d\ell^* - d\ell}{d\ell} = EA \left( \frac{d\ell^*}{d\ell} - 1 \right) \tag{10}$$

where  $E$  is the Young's modulus,  $A$  is the area of the cable section in the unstrained configuration. Employing Eq. (5b), one gets:

$$\frac{d\ell^*}{d\ell} = \frac{ds^*}{ds} = \chi t(s) + 1 \tag{11}$$

where

$$\chi = \frac{pL}{EA} \tag{12}$$

Resorting to chain rule of differentiation,  $d\xi/ds = (d\xi/ds^*)(ds^*/ds)$ , and according to Eqs. (8) and (11), the following equation is derived:

$$\frac{d\xi(s)}{ds} = \frac{\mathbf{t}(s)}{t(s)} [\chi t(s) + 1] = \chi(\mathbf{r} - \boldsymbol{\pi}s) + \frac{\mathbf{r} - \boldsymbol{\pi}s}{\|\mathbf{r} - \boldsymbol{\pi}s\|} \tag{13}$$

The sought solution is obtained by integrating the previous equation:

$$\xi(s) = \chi \int \mathbf{t}(s) ds + \int \frac{\mathbf{t}(s)}{t(s)} ds = \chi \int (\mathbf{r} - \pi s) ds + \int \frac{\mathbf{r} - \pi s}{\|\mathbf{r} - \pi s\|} ds \tag{14}$$

While the first integral can be easily solved, the second one requires some manipulations, which are reported in Appendix A. Finally, introducing the operator

$$\rho(\bullet) = \|\mathbf{r} - (\bullet)\| - \pi^T [\mathbf{r} - (\bullet)] \tag{15}$$

one gets

$$\xi(s) = \chi \left( \mathbf{r} s - \pi \frac{s^2}{2} \right) + (\mathbf{I} - \pi \pi^T) \mathbf{r} \ln[\rho(\pi s)] - \pi \|\mathbf{r} - \pi s\| + \mathbf{c} \tag{16}$$

where  $\mathbf{I}$  is the identity matrix of order three. The constant vector  $\mathbf{c}$  is determined by imposing the coordinates of cable origin,  $\xi(0)$ , so that Eq. (16) is rewritten as follows:

$$\xi(s) = \chi \left( \mathbf{r} s - \pi \frac{s^2}{2} \right) + (\mathbf{I} - \pi \pi^T) \mathbf{r} \ln \left[ \frac{\rho(\pi s)}{\rho(\mathbf{0})} \right] - \pi (\|\mathbf{r} - \pi s\| - \|\mathbf{r}\|) + \xi(0) \tag{17}$$

The unknown vector  $\mathbf{r}$  must be evaluated imposing the coordinates at cable end point,  $\xi(1)$ , by employing a numerical method such as Newton–Raphson. Once  $\mathbf{r}$  has been calculated, the elastic catenary is cast in closed form by Eq. (17) and the segment cable length in the stretched configuration can be evaluated by means of Eq. (11), so to read:

$$\ell^* = L s^*(s) = L \int_0^s (\chi t(s) + 1) ds \tag{18}$$

When Eq. (17) is written for plane problems it reduces to that proposed by Irvine (1981), as will be shown in Section 6.

### 3. Additional one point force

Let us assume that one point force  $\mathbf{P}$  acts on the cable. The equilibrium Eq. (1) can be redefined as:

$$\mathbf{t}(s) = t(s) \frac{d\xi(s)}{ds^*} = \mathbf{r} - \mathbf{f} U(s - \bar{s}) - \pi s \tag{19}$$

where  $\mathbf{f} = \mathbf{P}/(pL)$  is the dimensionless point force applied at abscissa  $\bar{s}$  and  $U(\cdot)$  is the unitary step function. For  $s \leq \bar{s}$  the solution reduces to that for cables with distributed load only, Eq. (17).

For  $\bar{s} < s \leq 1$  the solution is given by the following expression:

$$\xi(s) = \chi \int_{\bar{s}}^s [\mathbf{r} - \mathbf{f} - \pi s] ds + \int_{\bar{s}}^s \frac{\mathbf{r} - \mathbf{f} - \pi s}{\|\mathbf{r} - \mathbf{f} - \pi s\|} ds + \xi(\bar{s}) \tag{20}$$

where  $\xi(\bar{s})$  is given by Eq. (17) with  $s = \bar{s}$ . The first integral can easily be solved, the second one is evaluated according to Eq. (A.7) in the Appendix A, by replacing  $\mathbf{r}$  with  $\mathbf{r} - \mathbf{f}$ , so that:

$$\xi(s) = \chi \left[ (\mathbf{r} - \mathbf{f})(s - \bar{s}) - \pi \frac{(s^2 - \bar{s}^2)}{2} \right] + (\mathbf{I} - \pi \pi^T) (\mathbf{r} - \mathbf{f}) \times \ln \left[ \frac{\rho(\mathbf{f} + \pi s)}{\rho(\mathbf{f} + \pi \bar{s})} \right] - \pi (\|\mathbf{r} - \mathbf{f} - \pi s\| - \|\mathbf{r} - \mathbf{f} - \pi \bar{s}\|) + \xi(\bar{s}) \tag{21}$$

Finally, by introducing the explicit expression of  $\xi(\bar{s})$ :

$$\xi(s) = \chi \left( \mathbf{r} s - \mathbf{f}(s - \bar{s}) - \pi \frac{s^2}{2} \right) + (\mathbf{I} - \pi \pi^T) \left\{ \mathbf{r} \ln \left[ \frac{\rho(\pi \bar{s}) \rho(\mathbf{f} + \pi s)}{\rho(\mathbf{0}) \rho(\mathbf{f} + \pi \bar{s})} \right] - \mathbf{f} \ln \left[ \frac{\rho(\mathbf{f} + \pi s)}{\rho(\mathbf{f} + \pi \bar{s})} \right] \right\} - \pi (\|\mathbf{r} - \mathbf{f} - \pi s\| + \|\mathbf{r} - \pi \bar{s}\| - \|\mathbf{r}\| - \|\mathbf{r} - \mathbf{f} - \pi \bar{s}\|) + \xi(0) \tag{22}$$

The unknown vector  $\mathbf{r}$  must be evaluated imposing the coordinates at cable end.

### 4. General solution for many point forces

The general case with many point forces arbitrarily oriented and constant distributed load is now considered exploiting the solution derived in Section 3.

With reference to Fig. 2, assume that the dimensionless point forces  $\mathbf{f}_i = \mathbf{P}_i/(pL)$  are applied at points  $s_i$ . For the first interval,  $0 \leq s \leq s_1$ , Eq. (17) still applies. For the generic cable intervals,  $s_i < s \leq s_{i+1}$ , provided that  $s_{N+1} = 1$ ,  $s_0 = 0$ ,  $\mathbf{F}_i = \sum_{j=0}^i \mathbf{f}_j$  and  $\mathbf{f}_0 = \mathbf{0}$ , the solution is written as follows:

$$\xi(s) = \chi \int_{s_i}^s [\mathbf{r} - \mathbf{F}_i - \pi s] ds + \int_{s_i}^s \frac{\mathbf{r} - \mathbf{F}_i - \pi s}{\|\mathbf{r} - \mathbf{F}_i - \pi s\|} ds + \xi(s_i) \tag{23}$$

where  $\xi(s_i)$  is the solution at the end of the previous interval. According to Eq. (A.7), the solution of Eq. (23) is:

$$\xi(s) = \chi \left[ (\mathbf{r} - \mathbf{F}_i)(s - s_i) - \pi \frac{(s^2 - s_i^2)}{2} \right] + (\mathbf{I} - \pi \pi^T) (\mathbf{r} - \mathbf{F}_i) \times \ln \left[ \frac{\rho(\mathbf{F}_i + \pi s)}{\rho(\mathbf{F}_i + \pi s_i)} \right] - \pi (\|\mathbf{r} - \mathbf{F}_i - \pi s\| - \|\mathbf{r} - \mathbf{F}_i - \pi s_i\|) + \xi(s_i) \tag{24}$$

Exploiting the recurrence relation between  $\xi(s_i)$  and  $\xi(s_{i-1})$ , i.e. the solutions at the end of two contiguous intervals, and assuming  $\mathbf{F}_{-1} = \mathbf{F}_0 = \mathbf{0}$  and  $s_{i+1} = s$ , after some manipulation one gets:

$$\xi(s) = \chi \left( \mathbf{r} s - \mathbf{F}_i s + \sum_{j=0}^i \mathbf{f}_j s_j - \pi \frac{s^2}{2} \right) + (\mathbf{I} - \pi \pi^T) \sum_{j=0}^i \left( (\mathbf{r} - \mathbf{F}_j) \ln \left[ \frac{\rho(\mathbf{F}_j + \pi s_{j+1})}{\rho(\mathbf{F}_j + \pi s_j)} \right] \right) - \pi \left[ \|\mathbf{r} - \mathbf{F}_i - \pi s\| - \|\mathbf{r}\| + \sum_{j=0}^i (\|\mathbf{r} - \mathbf{F}_{j-1} - \pi s_j\| - \|\mathbf{r} - \mathbf{F}_j - \pi s_j\|) \right] + \xi(0) \tag{25}$$

Eq. (25) applies to all cable segments, for the first segment (from cable origin to the first force) it will be  $i = 0$ , whereas for the last segment (from the last force to cable end)  $i = N$ .

The vector  $\mathbf{r}$  is evaluated setting  $i = N$  and imposing the coordinates at cable end. The implementation of Eq. (25) in a numerical procedure is straightforward. All the calculations which will be shown in the following have been performed by means of Mathematica®.

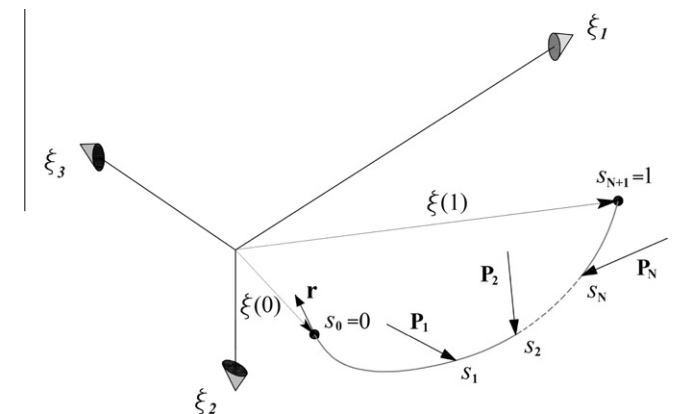


Fig. 2. Forces acting on the cable in the dimensionless coordinate system.

### 5. Thermal loads

In real applications the effect of thermal loads on the cable should be taken into account. For example, during suspension bridge erection stages the effect of thermal loads can be decisive for the correct prediction of the geometry of the bridge in the final configuration.

The thermal load can be easily added in the formulation by considering the total strain as the superposition of the elastic and thermal contributions:

$$\frac{ds^* - ds}{ds} = \chi t(s) + \alpha \Delta\theta \tag{26}$$

in which  $\alpha$  is the linear thermal expansion coefficient and  $\Delta\theta$  the temperature jump. Eq. (23) is modified as follows:

$$\xi(s) = \chi \int_{s_i}^s [\mathbf{r} - \mathbf{F}_i - \boldsymbol{\pi}s] ds + (1 + \alpha \Delta\theta) \int_{s_i}^s \frac{\mathbf{r} - \mathbf{F}_i - \boldsymbol{\pi}s}{\|\mathbf{r} - \mathbf{F}_i - \boldsymbol{\pi}s\|} ds + \xi(s_i) \tag{27}$$

The related solution is easily derived by suitable modification of Eq. (25).

### 6. Model validation

The model herein derived is consistent with the classical derivation of the elastic catenary. Indeed, if we consider only a vertical uniformly distributed load, it follows that  $\boldsymbol{\pi} = [0, 1, 0]^T$  and  $\mathbf{r} = [r_{x_1}, r_{x_2}, r_{x_3}]^T \equiv [r_{x_1}, r_{x_2}, 0]^T$ . In Eq. (17),  $(\mathbf{I} - \boldsymbol{\pi}\boldsymbol{\pi}^T)\mathbf{r} = [r_{x_1}, 0, 0]^T$  and the two non-nil components of Eq. (17) reduce to:

$$\xi_1(s) = \chi r_{x_1} s + r_{x_1} \ln \left[ \frac{\sqrt{r_{x_1}^2 + (r_{x_2} - s)^2} - r_{x_2} + s}{\sqrt{r_{x_1}^2 + r_{x_2}^2} - r_{x_2}} \right] \tag{28}$$

$$\xi_2(s) = \chi \left( r_{x_2} s - \frac{s^2}{2} \right) - \left( \sqrt{r_{x_1}^2 + (r_{x_2} - s)^2} - \sqrt{r_{x_1}^2 + r_{x_2}^2} \right) \tag{29}$$

where it has been assumed  $\xi(0) = [0, 0, 0]^T$ . The quantity  $\beta = r_{x_2}/r_{x_1}$  is the ratio between vertical and horizontal components of cable tension at first cable end. When supports are at the same level,  $\beta$  coincides with the classical catenary parameter. With some manipulation (see Appendix B), Eq. (28) can be rewritten as follows:

$$\xi_1(s) = \chi r_{x_1} s + r_{x_1} \left[ \sinh^{-1} \left( \frac{r_{x_2}}{r_{x_1}} \right) - \sinh^{-1} \left( \frac{r_{x_2} - s}{r_{x_1}} \right) \right] \tag{30}$$

As in Irvine (1981), the apex “-1” means inverse hyperbolic function. If we substitute dimensional quantities, Eqs. (29) and (30) coincide with those reported by Irvine (1981).

In order to validate the out of plane solution, a cable suspended between supports at the same level has been considered, with  $EA = 1.5708 \cdot 10^9$  N,  $L = 220$  m,  $\mathbf{x}_0 = [0, 0, 0]^T$  and  $\mathbf{x}_L = [100, 0, 0]^T$ . The uniformly distributed vector load is  $\mathbf{p} = 616.538[0, \sqrt{3}/2, 1/2]^T$  N/m, forming an angle of  $30^\circ$  with the vertical axis. The solution by Eq. (17) gives  $\mathbf{R} = [13163.2, 58733.1, 33909.6]^T$  N. Adopting the classic catenary solution, given by Eqs. (29) and (30), with a vertical load  $\|\mathbf{p}\| = 616.538$  N/m, the solution is  $R_{x_1} = 13163.2$  N and  $R_{x_2} = 67819.1$  N. This solution coincides with the previous one albeit in a rotated reference system.

It is interesting to note that in the case of a non-heavy elastic cable, subjected to  $N$  point forces, in the interval  $\ell_i < \ell \leq \ell_{i+1}$ , the following funicular of forces can be easily obtained:

$$\mathbf{x}(\ell) = \frac{1}{EA} \left( \mathbf{R}\ell - \sum_{j=0}^i \mathbf{P}_j(\ell - \ell_j) \right) + \sum_{j=0}^i \frac{\mathbf{R} - \sum_{k=0}^j \mathbf{P}_k}{\|\mathbf{R} - \sum_{k=0}^j \mathbf{P}_k\|} (\ell_{j+1} - \ell_j) + \mathbf{x}(0), \tag{31}$$

in which  $\ell_{N+1} = \ell$  and the quantities with nil pedix are set to zero. This equation simply states that the final position of a point of the cable at abscissa  $\ell$  is the sum of the elastic contribution of the various segments, plus the initial position. It can be used to validate Eq. (25), which must give the same result of Eq. (31) as the distributed load vanishes. To this aim, the same cable of the previous example has been considered, loaded with four point forces  $\mathbf{P}_1 = [50, 0, 0]^T$  kN,  $\mathbf{P}_2 = [0, 50, 0]^T$  kN,  $\mathbf{P}_3 = [0, 0, 50]^T$  kN,  $\mathbf{P}_4 = \frac{1}{\sqrt{3}}[50, 50, 50]^T$  kN applied, respectively at  $\ell_1 = L/5$ ,  $\ell_2 = 2L/5$ ,  $\ell_3 = 3L/5$ ,  $\ell_4 = 4L/5$ . An initial distributed load  $\mathbf{p} = [0, 10, 0]^T$  kN has also been applied. When the distributed load vanishes, Eq. (25) must give the same numerical solution of Eq. (31). In order to check the validity of the model, the coordinates, in the stretched configuration, of the first forced point ( $\ell_1 = L/5$ ) have been chosen as control parameters. Table 1 shows that the solution by the proposed model approaches that obtained by the funicular method as the distributed load decreases from  $\mathbf{p}$  to  $10^{-5}\mathbf{p}$ . Fig. 3 shows the sequence of deformed shapes of the cable when the distributed load  $\mathbf{p}$  decreases.

### 7. Numerical applications

The effectiveness of the proposed formulation is tested with respect to two example problems: a three dimensional cable system with spring and a transport pulley system. For each of them two different settings are considered. The first one involves cable stretched configurations on the vertical planes, for which 2D equilibrium formulation are suitable, and is aimed to test the solution with those available in the literature. The second setting highlights the versatility of the procedure to handle 3D stretched configurations.

Each problem is modeled by a system of equilibrium equations derived from Eq. (17) or Eq. (25) and enforcing the proper boundary conditions, which will be reported in dimensional form.

#### 7.1. Three dimensional cable system with spring

The three degrees of freedom structure, depicted in Fig. 4, consisting of three cables jointly supported by a vertical spring, the end of which freely rolls horizontally, has been addressed by Such et al. (2009), Huang and Lan (2006), Peyrot and Goulois (1979). The elastic cables have axial stiffness  $EA = 2.910^5$  N and are joined at the same point A of coordinates  $\mathbf{x}_A = [400, 0, 300]$  m which is connected to a vertical spring of stiffness  $\mathbf{k} = [0, 1000, 0]$  N/m. Unstrained cable lengths are  $L^{(1)} = 580$  m and  $L^{(2)} = L^{(3)} = 510$  m, cable weights are  $\mathbf{p}^{(1)} = [0, 1, 0]^T$  N/m and  $\mathbf{p}^{(2)} = \mathbf{p}^{(3)} = [0, 2, 0]^T$  N/m, where the apex identifies the cable. A horizontal force  $\mathbf{F} = [0, 0, -1000]$  N is applied in A, furthermore the cables, with

**Table 1**  
Cable of Section 6 subjected to four point forces. Coordinates of the first forced point decreasing the distributed load, derived by Eq. (25) and without distributed load, derived by Eq. (31).

	$p_{x_2}$ (kN)	$x_1(\ell_1)$ (m)	$x_2(\ell_1)$ (m)	$x_3(\ell_1)$ (m)
Eq. (25)	10	12.536	42.162	0.871
	1	23.540	36.644	5.973
	0.1	34.872	23.942	12.111
	0.01	36.485	20.855	13.041
	0.001	36.646	20.514	13.133
	0.0001	36.661	20.480	13.142
Eq. (31)	0	36.663	20.476	13.143

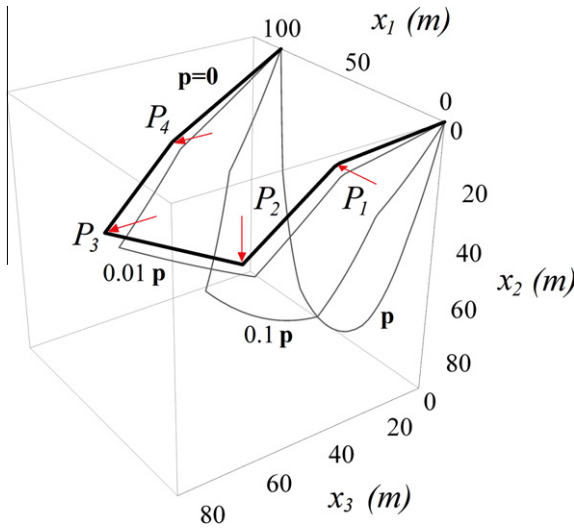


Fig. 3. Deformed shape of a cable under a uniformly distributed vertical load  $\mathbf{p}$ ,  $0.1\mathbf{p}$ ,  $0.01\mathbf{p}$ ,  $0.001\mathbf{p}$  and four point forces (gray lines) compared with the funicular of point forces, i.e. the deformed shape for  $\mathbf{p} = \mathbf{0}$  (black line).

coefficient of thermal expansions  $\alpha = 6.510^{-6} \text{ } ^\circ\text{C}^{-1}$ , are subjected to a temperature increment  $\Delta\theta = 100^\circ\text{C}$ . The coordinates of the initial point of the cables are the following:  $\mathbf{x}_0^{(1)} = [800, 400, 300]^T \text{ m}$ ,  $\mathbf{x}_0^{(2)} = [0, 0, 0]^T \text{ m}$ ,  $\mathbf{x}_0^{(3)} = [0, 0, 600]^T \text{ m}$ . Eq. (17) must be imposed for each cable, besides the thermal load is considered as shown in Eq. (27). The following boundary conditions apply:

$$\mathbf{x}^{(1)}(L^{(1)}, \mathbf{R}^{(1)}) = \mathbf{x}^{(2)}(L^{(2)}, \mathbf{R}^{(2)}) \quad (32)$$

$$\mathbf{x}^{(3)}(L^{(3)}, \mathbf{R}^{(3)}) = \mathbf{x}^{(2)}(L^{(2)}, \mathbf{R}^{(2)}) \quad (33)$$

$$\sum_{i=1}^3 (\mathbf{R}^{(i)} - \mathbf{p}^{(i)}L^{(i)}) + \mathbf{F} + \mathbf{k}[\mathbf{x}_2^{(1)}(L^{(1)}) - \mathbf{x}_{2,A}] = \mathbf{0} \quad (34)$$

Eqs. (32) and (33) account for displacement constraint of cable ends; Eq. (34) states the force equilibrium of node A in the global reference system. These constitutes a set of 9 non-linear equations, equal to the number of unknown quantities given by the components of vectors  $\mathbf{R}^{(i)}$ , which can be easily solved by choosing a suitable initial value. The convergence to the unique solution is very fast. For example, given as initial guess  $\mathbf{R}^{(1)} = [-100, -100, -100]^T \text{ N}$ ,  $\mathbf{R}^{(2)} = [100, 100, 100]^T \text{ N}$ ,  $\mathbf{R}^{(3)} = [100, 100, -100]^T \text{ N}$ , 13 iterations are needed by a Newton algorithm.

As a comparison, Table 2 lists the displacements of point A as reported by Such et al. (2009), Huang and Lan (2006), Peyrot and Goulois (1979), along with those given by the proposed formulation. Fig. 5a shows the stretched configuration of the cables along with the unstrained one; as expected the load conditions are such that each cable maintains a vertical planar layout.

The procedure is now tested adding to previous loads a wind action causing non-vertical cable layout, which cannot be reproduced analytically by existing formulations, unless a different reference system is chosen for each cable. Let us suppose that a horizontal distributed load along  $x_3$ , due to wind, is applied to the three cables. As the cable is slightly extensible, for the sake of the example the load can be applied to the unstrained configuration and roughly approximated as uniformly distributed and equal to  $p_{x_3} = 0.5\rho_a c_D b U^2$ , where  $\rho_a = 1.25 \text{ kg/m}^3$  is air density,  $c_D = 1.2$  is the drag coefficient,  $b = 0.01 \text{ m}$  is the diameter of the cables,  $U = 20 \text{ m/s}$  is the mean flow velocity. The distributed loads modify as follows:  $\mathbf{p}^{(1)} = [0, 1, 3]^T \text{ N/m}$  and  $\mathbf{p}^{(2)} = \mathbf{p}^{(3)} = [0, 2, 3]^T \text{ N/m}$ . The deformed shape is plotted in Fig. 5b and the displacement of point A

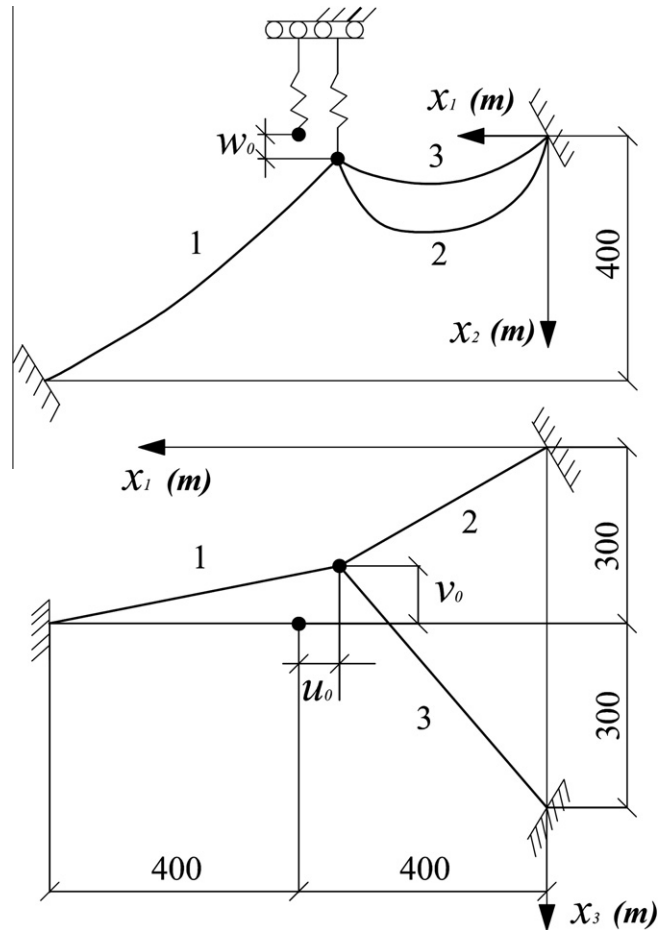


Fig. 4. Cable system with a spring.

is reported in Table 2. The guess solution is chosen with vertical reaction components opposite to self weight and along  $x_3$  components opposite to wind action. If  $\mathbf{R}^{(1)} = [-100, 100, 100]^T \text{ N}$ ,  $\mathbf{R}^{(2)} = \mathbf{R}^{(3)} = [100, 100, 100]^T \text{ N}$  are chosen as initial guess, 9 iterations are required.

### 7.2. Transport pulley system

The static behavior of a cable system supported by a pulley was studied by Such et al. (2009) and Bruno and Leonardi (1999) in order to model ski lifts, electrical transmission lines and cable systems in erection procedures of long-span bridges. The example

Table 2  
Displacement at point A of the cable system with spring by different approaches.

	$u_0 \equiv x_{1,A} - x_1^{(1)}(L^{(1)})$	$v_0 \equiv x_{3,A} - x_3^{(1)}(L^{(1)})$	$w_0 \equiv x_{2,A} - x_2^{(1)}(L^{(1)})$
Proposed method	26.471	41.138	-2.875
Peyrot and Goulois (1979)	26.473	41.135	-2.874
Huang and Lan (2006)	26.471	41.138	-2.874
Such et al. (2009)	26.527	41.105	-2.883
With horizontal distributed load:			
Proposed method	23.676	-40.468	-3.756

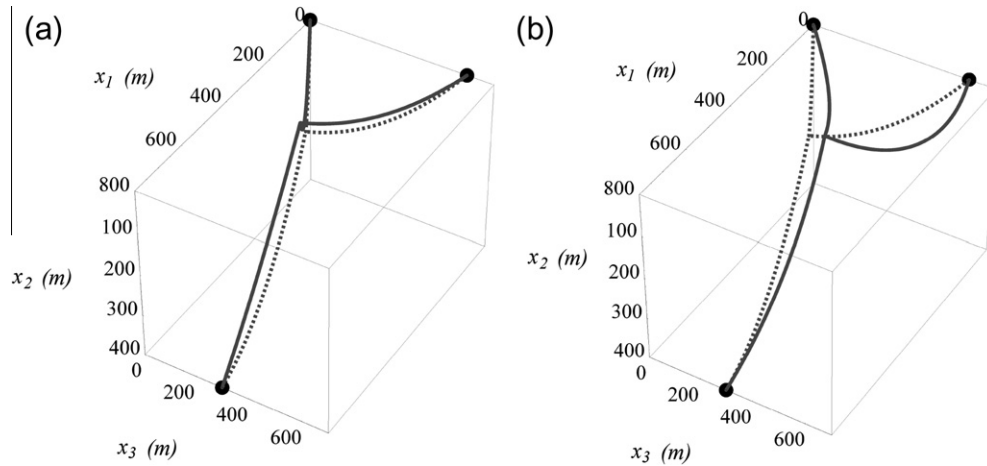


Fig. 5. Unstrained (dotted line) and stretched (solid line) configuration of the cable system with a spring: (a) without wind force; (b) with wind force.

discussed by Such et al. (2009) and Bruno and Leonardi (1999), see Fig. 6, contemplates only planar stretched configuration and refers to a cable with initial length  $L = 500$  m, Young's modulus  $E = 16$  GPa, cross section area  $A = 8.05 \cdot 10^{-4}$  m<sup>2</sup>, linear density  $m = 6.327$  kg/m, linear weight  $p_x = 62.0679$  N/m. The cable ends are fixed at point 1 with coordinates  $\mathbf{x}_0 = [0, 0, 0]^T$  m and at point 2 with coordinates  $\mathbf{x}_L = [300, -50, 0]^T$  m. A frictionless pulley located at  $x_2 = -100$  m is let to move horizontally along  $x_1$ .

Such et al. (2009) seek for the equilibrium configurations of the cable under the assumption that the pulley is free to move horizontally (i.e. it gives only a vertical force to the cable) and its radius is negligible. Two equilibrium configurations were detected in the paper, named  $C_1$  and  $C_2$  in Fig. 6. The authors state that their formulation needs 15 equations to find the equilibrium configurations. Bruno and Leonardi (1999) consider a more realistic pulley whose radius is taken into account by adding some geometrical parameters. For the problem under investigation the pulley radius was set equal to 0.30 m. Considering that the pulley radius is very small in comparison with cable length  $L$ , it is not surprising that the equilibrium configurations detected by Bruno and Leonardi (1999) basically coincide with those reported by Such et al. (2009).

Bruno and Leonardi (1999) also consider an auxiliary problem where the pulley is now restrained at its position  $x_1$  which is treated as a variable quantity (i.e. the pulley has vertical and horizontal

reactions). An equilibrium path varying the pulley position  $x_1$  is reported in the paper.

Let us tackle the problem by means of the formulation proposed herein, taking advantage of Eq. (22). When the pulley is free to move along  $x_1$ , the point load  $\mathbf{P} = [0, P, 0]^T$  (i.e. the reaction of the pulley) and its abscissa  $\bar{\ell}$  are considered as unknown quantities. The solution is obtained by satisfying the following set of equations:

$$\mathbf{x}(L, \mathbf{R}, \mathbf{P}) = \mathbf{x}_L \quad (35)$$

$$x_2(\bar{\ell}, \mathbf{R}, \mathbf{P}) = -100 \quad (36)$$

$$2(R_{x_2} - p_{x_2} \bar{\ell}) = P \quad (37)$$

As regards the boundary conditions (35), only the two equations related to directions  $x_1$  and  $x_2$  are meaningful, as the cable layout is in the  $x_1 - x_2$  plane. Eq. (36) sets pulley height; Eq. (37) matches the tension at both sides of the frictionless pulley. Thus, 4 equations with the unknowns  $R_{x_1}$ ,  $R_{x_2}$ ,  $P$ ,  $\bar{\ell}$  define the problem.

The two stable equilibrium configurations  $C_1$  and  $C_2$  have been correctly find out by the proposed formulation. A third equilibrium configuration  $C_3$  (see Fig. 6), not reported in previous literature, has also been spotted, although of unstable nature. Table 3 compares the curvilinear pulley abscissa at equilibrium and cable tension at pulley location with those given by Such et al. (2009) and Bruno and Leonardi (1999), denoting with  $a_g$  the acceleration due to gravity. The guess values  $P = -25$  kN,  $\mathbf{R} = [2.5, 3.5, 0]^T$  kN,  $\bar{\ell} = 80$  m, have been adopted in order to find the first equilibrium point;  $P = -35$  kN,  $\mathbf{R} = [2.5, 3.5, 0]^T$  kN,  $\bar{\ell} = 300$  m for the second equilibrium point;  $P = -25$  kN,  $\mathbf{R} = [2.5, 3.5, 0]^T$  kN,  $\bar{\ell} = 120$  m for the third equilibrium point. The required iterations were respectively 7, 5, 6.

The auxiliary problem with the pulley restrained at position  $x_1$  has also been investigated. The pulley is supposed fixed at  $\mathbf{x}_P = [x_1, -100, 0]^T$  m, the load is redefined as  $\mathbf{P} = [P_{x_1}, P_{x_2}, 0]^T$ . The following set of equations has been iteratively solved, varying the pulley coordinate  $x_1$ :

$$\mathbf{x}(L, \mathbf{R}, \mathbf{P}) = \mathbf{x}_L \quad (38)$$

$$\mathbf{x}(\bar{\ell}, \mathbf{R}, \mathbf{P}) = \mathbf{x}_P \quad (39)$$

$$\|\mathbf{R} - \mathbf{p}\bar{\ell}\| = \|\mathbf{R} - \mathbf{P} - \mathbf{p}\bar{\ell}\| \quad (40)$$

which define 5 meaningful equations with unknowns  $R_{x_1}$ ,  $R_{x_2}$ ,  $P_{x_1}$ ,  $P_{x_2}$ ,  $\bar{\ell}$ .

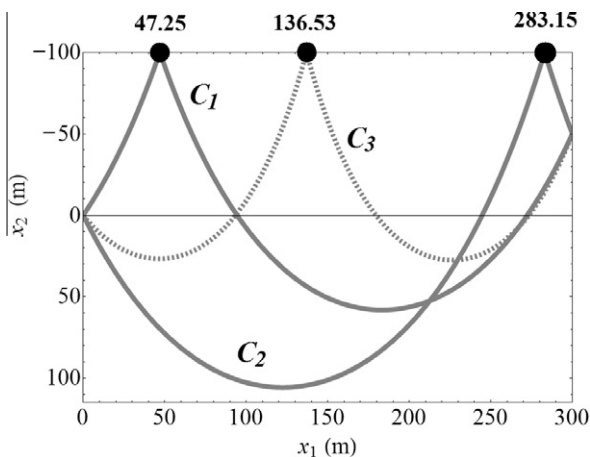


Fig. 6. Stable (solid) and unstable (dashed) equilibrium configurations of the cable system supported by a pulley located at  $x_2 = -100$  m and free to move in the direction  $x_1$ .

**Table 3**  
Curvilinear pulley abscissa at equilibrium and cable tension at pulley location for the plane cable supported by a pulley free to move in the direction  $x_1$ .

	Bruno and Leonardi (1999)	Such et al. (2009)	Proposed method
<i>First equilibrium configuration</i>			
$\bar{\ell}$ (m)	111.07	110.96	110.833
$T(\bar{\ell})/a_g$ (kg)	1478.00	1481.23	1481.23
<i>Second equilibrium configuration</i>			
$\bar{\ell}$ (m)	446.37	446.92	447.295
$T(\bar{\ell})/a_g$ (kg)	1830.00	1831.40	1833.02
<i>Third equilibrium configuration (unstable)</i>			
$\bar{\ell}$ (m)	-	-	221.518
$T(\bar{\ell})/a_g$ (kg)	-	-	1083.68

Fig. 7 shows the continuous equilibrium path representing the value of the horizontal pulley reaction  $P_{x_1}$  versus the pulley location  $x_1$  at equilibrium configurations, i.e. the horizontal force arising at the pulley imposing its position. Unstable solutions are symbolized by the dashed line, whereas the solid line stands for stable configurations. In order to assess the type of equilibrium,

the total potential energy of the cable has been evaluated. Fig. 8 shows the equilibrium configurations for the scenarios marked in Fig. 7.

The equilibrium points referenced to a pulley free to move are detected from Fig. 7 as those for which  $P_{x_1} \equiv 0$ : point  $a$  identifies the stable configuration  $C_1$ , point  $f$  identifies the stable configuration  $C_2$ , point  $d_2$  identifies the unstable configuration  $C_3$ . Fig. 7 shows that if the pulley is fixed in the range  $100.62 \text{ m} < x_1 < 147.00 \text{ m}$ , three equilibrium configurations are possible, one is unstable the others are stable; then two cable layouts are possible for a given pulley position. If the cable layout is perturbed or it is that of an unstable configuration, the cable slips so to assume a stable layout. If the pulley is fixed at a position with  $x_1 < 100.62 \text{ m}$  or  $x_1 > 147.00 \text{ m}$  a single stable solution is possible.

Alternatively, one can impose the force at the pulley, free to move along direction  $x_1$ , and register its displacement. For example, if one increases the horizontal force applied to the pulley, starting from the first equilibrium point (point  $a$ ) so to move it to the right (toward point  $f$ ), then once that point  $c_1$  is reached a snap through instability phenomenon is encountered and the pulley rapidly moves to point  $g$ .

The equilibrium path reported by Bruno and Leonardi (1999) did not evidence the unstable branch and presents a discontinuity, maybe due to lack of convergence, which is not encountered in the present analysis.

The analysis has been repeated for a spatial cable system with non-planar cable layout, where the pulley is let to move on the new horizontal line with  $x_2 = -100 \text{ m}$  and  $x_3 = 50 \text{ m}$ . When the pulley is free to move along  $x_1$ , three equilibrium configurations are detected, as in the previous case, and reported in Fig. 9. The guess values  $\mathbf{P} = [0, -27, 1]^T \text{ kN}$ ,  $\mathbf{R} = [4.8, -6.9, 0]^T \text{ kN}$ ,  $\bar{\ell} = 100 \text{ m}$ , have been adopted in order to find the first equilibrium point;  $\mathbf{P} = [0, -30, 10]^T \text{ kN}$ ,  $\mathbf{R} = [5, 10, 1]^T \text{ kN}$ ,  $\bar{\ell} = 450 \text{ m}$  for the second equilibrium point;  $\mathbf{P} = [0, -20, 2]^T \text{ kN}$ ,  $\mathbf{R} = [2, 4, 1]^T \text{ kN}$ ,  $\bar{\ell} = 260 \text{ m}$  for the third equilibrium point. The required iterations were respectively 6, 5, 6. The equilibrium path related to the case with the pulley restrained at position  $x_1$ , plotted in Fig. 10, assesses that the cable behavior is analogous to the companion plane problem. The curvilinear pulley abscissa at equilibrium is reported in Table 4, along with cable tension at pulley location, denoting with  $a_g$  the acceleration due to gravity.

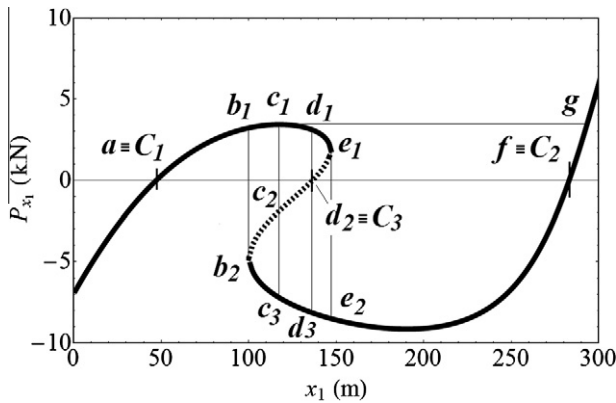


Fig. 7. Equilibrium path of plane cable with pulley: horizontal pulley reaction  $P_{x_1}$  versus pulley location  $x_1$  for stable (solid line) and unstable (dashed line) equilibrium.

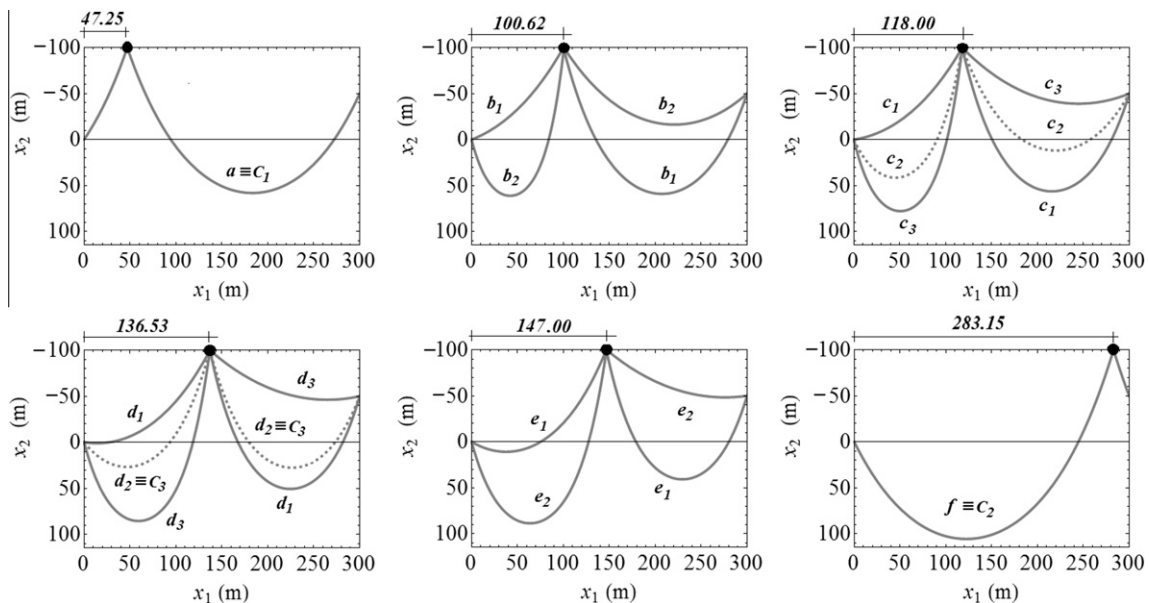


Fig. 8. Stable (solid line) and unstable (dashed line) equilibrium configurations of the plane cable pulley system for the settings evidenced in Fig. 6.

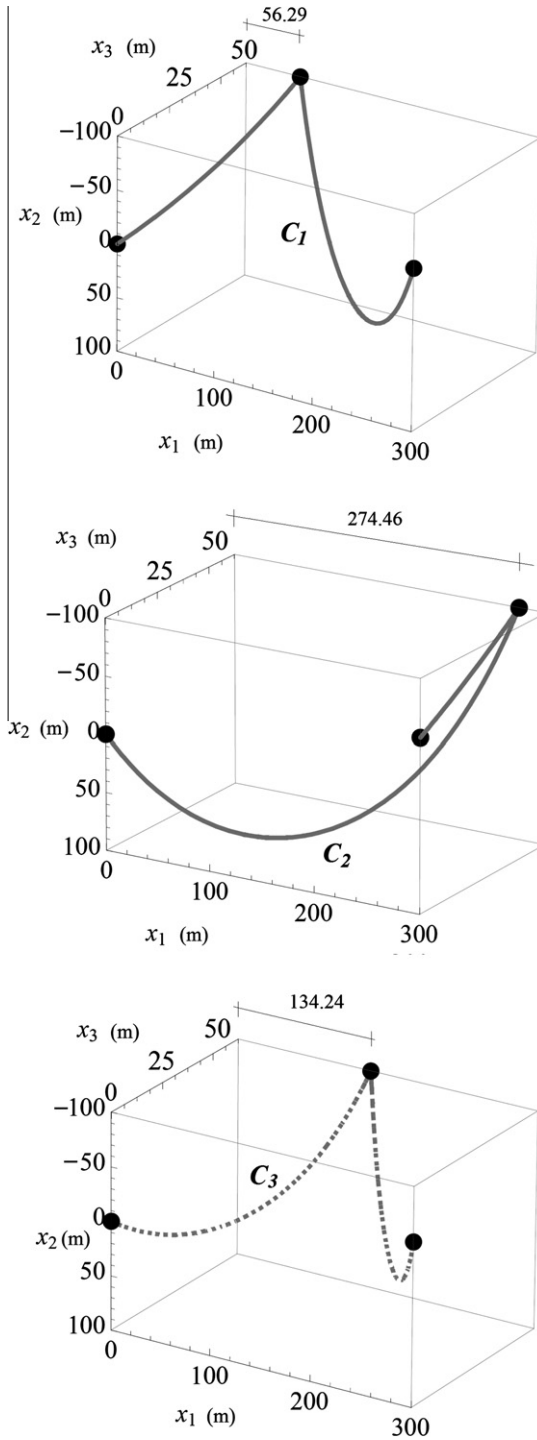


Fig. 9. Equilibrium positions of cable with pulley in spatial configuration.

### 8. Conclusions

The paper presents a model for obtaining the deformed shape of an elastic cable under a uniformly distributed load and many point forces, generally oriented in space. The model differs from other approaches because the solution is given in a vector form, which reduces to that contained in classic literature when only vertical loads act on the cable. A remarkable closed form expression is proposed which is able to cope with a set of cables with many in-span point forces however oriented in space. A considerable advantage is related to the easiness of operating in a global reference system.

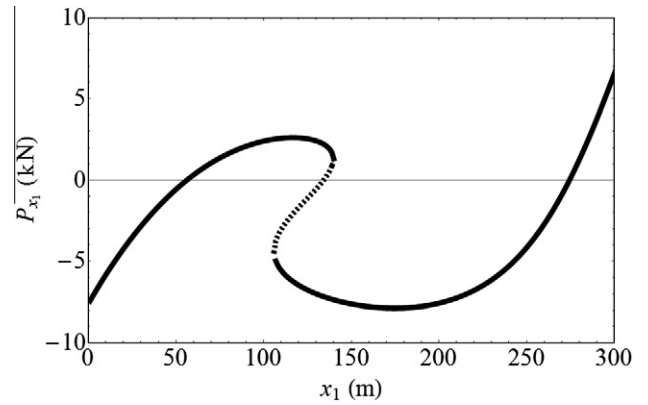


Fig. 10. Equilibrium path for 3D cable supported by a pulley.

Table 4

Curvilinear pulley abscissa at equilibrium and cable tension at pulley location for the 3D cable supported by a pulley free to move in the direction  $x_1$ .

	Proposed method
<i>First equilibrium configuration</i>	
$\bar{\ell}$ (m)	126.122
$T(\bar{\ell})/a_g$ (kg)	1439.66
<i>Second equilibrium configuration</i>	
$\bar{\ell}$ (m)	424.757
$T(\bar{\ell})/a_g$ (kg)	1775.31
<i>Third equilibrium configuration (unstable)</i>	
$\bar{\ell}$ (m)	219.983
$T(\bar{\ell})/a_g$ (kg)	1099.43

The capability to reproduce non-planar layouts under generic point forces represents a significant improvement with respect to existing approaches. Thermal loads may be considered too.

The model has been validated comparing the deformed shape under skew uniformly distributed load with that obtained by a classical formulation in a rotated reference system. Furthermore, when 3D point forces are introduced, the convergence of the limit case with vanishing distributed load to the funicular of forces has been verified.

As shown in the applications, the proposed formulation is well suited to be implemented for the numerical solution of complex cable problems.

### Appendix A

Scope of the appendix is to describe how the solution of the integral  $\int \frac{\mathbf{t}(s)}{t(s)} ds = \int \frac{\mathbf{r} - \boldsymbol{\pi}s}{t(s)} ds$  has been pursued.

Considering that  $\boldsymbol{\pi}$  is a versor then  $\boldsymbol{\pi}s = \boldsymbol{\pi} \boldsymbol{\pi}^T \boldsymbol{\pi}s$ , furthermore  $\boldsymbol{\pi}\boldsymbol{\pi}^T \mathbf{r} = \boldsymbol{\pi} \mathbf{r}^T \boldsymbol{\pi}$ , so that the integral can be written as:

$$\begin{aligned} \int \frac{\mathbf{t}(s)}{t(s)} ds &= \int \frac{\mathbf{r} - \boldsymbol{\pi}s}{t(s)} ds = \int \frac{\mathbf{r} - \boldsymbol{\pi}\boldsymbol{\pi}^T \mathbf{r} + \boldsymbol{\pi}\mathbf{r}^T \boldsymbol{\pi} - \boldsymbol{\pi}\boldsymbol{\pi}^T \boldsymbol{\pi}s}{t(s)} ds \\ &= (\mathbf{I} - \boldsymbol{\pi}\boldsymbol{\pi}^T) \mathbf{r} \int \frac{1}{t(s)} ds + \boldsymbol{\pi} \int \frac{\mathbf{t}^T(s) \boldsymbol{\pi}}{t(s)} ds \\ &= (\mathbf{I} - \boldsymbol{\pi}\boldsymbol{\pi}^T) \mathbf{r} \int \left(1 - \frac{\boldsymbol{\pi}^T \mathbf{t}(s)}{t(s)}\right) \frac{1}{t(s) - \boldsymbol{\pi}^T \mathbf{t}(s)} ds \\ &\quad + \boldsymbol{\pi} \int \frac{\mathbf{t}^T(s) \boldsymbol{\pi}}{t(s)} ds \end{aligned} \tag{A.1}$$

As the following relationship hold

$$\frac{dt(s)}{ds} = \frac{\mathbf{t}^T(s)}{t(s)} \frac{d\mathbf{t}(s)}{ds} = - \frac{\mathbf{t}^T(s) \boldsymbol{\pi}}{t(s)} \tag{A.2}$$

$$\frac{d\mathbf{t}(s)}{ds} = \frac{d}{ds}(\mathbf{r} - \boldsymbol{\pi}s) = -\boldsymbol{\pi} \quad (\text{A.3})$$

$$\frac{d}{ds}[t(s) - \boldsymbol{\pi}^T \mathbf{t}(s)] = -\frac{\mathbf{t}^T(s)\boldsymbol{\pi}}{t(s)} + \boldsymbol{\pi}^T \boldsymbol{\pi} = 1 - \frac{\mathbf{t}^T(s)\boldsymbol{\pi}}{t(s)} \quad (\text{A.4})$$

Eq. (A.1) can be cast in the following form

$$\int \frac{\mathbf{t}(s)}{t(s)} ds = (\mathbf{I} - \boldsymbol{\pi}\boldsymbol{\pi}^T)\mathbf{r} \int \frac{1}{t(s) - \boldsymbol{\pi}^T \mathbf{t}(s)} d[t(s) - \boldsymbol{\pi}^T \mathbf{t}(s)] - \boldsymbol{\pi} \int dt(s) \quad (\text{A.5})$$

The sought solution can be written as

$$\begin{aligned} \int \frac{\mathbf{t}(s)}{t(s)} ds &= (\mathbf{I} - \boldsymbol{\pi}\boldsymbol{\pi}^T)\mathbf{r} \ln[t(s) - \boldsymbol{\pi}^T \mathbf{t}(s)] - \boldsymbol{\pi} t(s) + \mathbf{c} \\ &= (\mathbf{I} - \boldsymbol{\pi}\boldsymbol{\pi}^T)\mathbf{r} \ln\|\mathbf{r} - \boldsymbol{\pi}s\| - \boldsymbol{\pi}^T(\mathbf{r} - \boldsymbol{\pi}s) - \boldsymbol{\pi}\|\mathbf{r} - \boldsymbol{\pi}s\| + \mathbf{c} \end{aligned} \quad (\text{A.6})$$

Introducing the operator defined by Eq. (15), one gets:

$$\int \frac{\mathbf{t}(s)}{t(s)} ds = (\mathbf{I} - \boldsymbol{\pi}\boldsymbol{\pi}^T)\mathbf{r} \ln[\rho(\boldsymbol{\pi}s)] - \boldsymbol{\pi}\|\mathbf{r} - \boldsymbol{\pi}s\| + \mathbf{c} \quad (\text{A.7})$$

## Appendix B

In order to show the equivalence between Eqs. (28) and (30), the equality

$$\ln\left[\sqrt{1 + \gamma^2} - \gamma\right] = -\sinh^{-1}\gamma \quad (\text{B.1})$$

is first proved. Indeed, making the position  $\gamma = \sinh\delta$ , the following manipulation clarify Eq. (B.1):

$$\begin{aligned} \ln\left[\sqrt{1 + \gamma^2} - \gamma\right] &= \ln\left[\sqrt{1 + \sinh^2\delta} - \sinh\delta\right] \\ &= \ln[\cosh\delta - \sinh\delta] = \ln e^{-\delta} = -\delta = -\sinh^{-1}\gamma \end{aligned} \quad (\text{B.2})$$

Thus, in Eq. (28):

$$\begin{aligned} \ln\left[\frac{\sqrt{r_{x_1}^2 + (r_{x_2} - s)^2} - r_{x_2} + s}{\sqrt{r_{x_1}^2 + r_{x_2}^2} - r_{x_2}}\right] &= \ln\left[\sqrt{1 + \left(\frac{r_{x_2} - s}{r_{x_1}}\right)^2} - \frac{r_{x_2} - s}{r_{x_1}}\right] \\ -\ln\left[\sqrt{1 + \frac{r_{x_2}^2}{r_{x_1}^2} - \frac{r_{x_2}}{r_{x_1}}}\right] &= -\sinh^{-1}\left(\frac{r_{x_2} - s}{r_{x_1}}\right) + \sinh^{-1}\left(\frac{r_{x_2}}{r_{x_1}}\right) \end{aligned} \quad (\text{B.3})$$

## References

- Andreu, A., Gil, L., Roca, P., 2006. A new deformable catenary element for the analysis of cable net structures. *Computers and Structures* 84 (29–30), 1882–1890.
- Bernoulli, J.M., 1691. Solutions to the problem of the catenary, or funicular curve. *Acta Eruditorum* (English Translation by Pierre Beaudry, *FIDELIO Magazine* (2001), 10(1)).
- Bernoulli, J., 1692. *Lectones mathematicae de methodo integralium*. In: *Lectures on the integral calculus*. *Acta Eruditorum*. (English Translation by William, A., Ferguson, Jr., 21st Century Science and Technology (2004), 17(1)).
- Bruno, D., Leonardi, A., 1999. Nonlinear structural models in cableway transport systems. *Simulation Practice and Theory* 7 (3), 207–218.
- Euler, L., 1744. *Methodus inveniendi lineas curvas*. Lausanna and Geneva.
- Galilei, G., 1638. *Discorsi e dimostrazioni matematiche intorno a due nuove scienze*. In: *Leida*.
- Hooke, R., 1675. *A description of heliostopes, and some other instruments*. John and Martin Printer to the Royal Society, London.
- Hooke, R., 1678. *Lectures de potentia restitutiva, or of spring explaining the power of springing bodies*. John and Martin Printer to the Royal Society, London.
- Huang, Y., Lan, W., 2006. Static analysis of cable structure. *Applied Mathematics and Mechanics* (English edition) 27 (10), 1425–1430.
- Irvine, H.M., 1981. *Cable Structures*. The MIT Press.
- Irvine, H.M., Sinclair, G.B., 1976. The suspended elastic cable under the action of concentrated vertical loads. *International Journal of Solids and Structures* 12 (4), 309–317.
- Kurrer, K.E., 2008. *The History of the Theory of Structures*. Ernst & Sohn, Berlin.
- Leibniz, G.W., 1691. Solutions to the Problem of the Catenary, or Funicular Curve, Proposed by Jacques, M., Bernoulli in the Acta of June 1691. *Acta Eruditorum*. (English Translation by Pierre Beaudry, *FIDELIO Magazine* (2001), 10(1)).
- Leibniz, G.W., 1691. The string whose curve is described by bending under its own weight, and the remarkable resources that can be discovered from it by however many proportional means and logarithms. *Acta Eruditorum*.
- Lepidi, M., Gattulli, V., Vestroni, F., 2007. Static and dynamic response of elastic suspended cables with damage. *International Journal of Solids and Structures* 44 (25–26), 8194–8212.
- Navier, M., 1823. *Rapport et memoire sur les ponts suspendus*, De L'imprimerie Royale, Paris.
- O'Brien, W.T., 1967. General solution of suspended cable system. *Journal of Structural Division – ASCE* 94, 1–26.
- Peyrot, A.H., Goulois, A.M., 1979. Analysis of cable structures. *Computer and Structures* 10 (5), 805–813.
- Such, M., Jimenez-Octavio, J.R., Carnicero, A., Lopez-Garcia, O., 2009. An approach based on the catenary equation to deal with static analysis of three dimensional cable structures. *Engineering Structures* 31 (9), 2162–2170.
- Timoshenko, S.P., 1983. *History of Strength of Materials*. Dover Publications.